Ceramics International xxx (xxxx) xxx–xxx

Contents lists available at ScienceDirect

Ceramics International

journal homepage: www.elsevier.com/locate/ceramint

Cation distributions and microwave dielectric properties of Cu-substituted $ZnGa_2O_4$ spinel ceramics

Xiaochi Lu[a,b], Wenjie Bian[a,b], Yaoyao Li[a,b], Haikui Zhu[a,b], Zhenxiao Fu[c], Qitu Zhang[a,*]

[a] College of Materials Science and Engineering, Nanjing Tech University, Nanjing 210009, China
[b] Jiangsu Collaborative Innovation Center for Advanced Inorganic Function Composites, 210009 Jiangsu, China
[c] Guangdong Fenghua Advanced Technology Company Limited, Zhaoqing 526020, Guangdong, China

ARTICLE INFO

Keywords:
$Zn_{1-x}Cu_xGa_2O_4$ ceramics
Spinel
Dielectric properties
Cation distribution

ABSTRACT

Spinel $Zn_{1-x}Cu_xGa_2O_4$ (x = 0–0.05) ceramics were prepared by the conventional solid-state method. Only a single phase was indexed in all samples. The relative density increased with Cu-substitution. Refined crystal structure parameters suggested that Cu^{2+} preferentially occupies the octahedron site and formed inverse spinel structure. The relative intensity of A^*_{1g} mode in Raman spectra confirmed that the inversion degree climbed with the growing content of Cu. The differences of ion dielectric polarizability resulted in the shift of absorption bands in Fourier transform infrared (FT-IR) spectroscopy. Ion dielectric polarizability and cell volumes differences affected permittivity (ε_r) and increased ε_r slightly during Cu-substitution. The temperature coefficient of resonant frequency (τ_f) kept steady, however, the quality factor ($Q \times f$) value of $Zn_{1-x}Cu_xGa_2O_4$ ceramics increased by 50% due to the Cu-substitution (from 85,824 GHz to 131,445 GHz). $Zn_{0.99}Cu_{0.01}Ga_2O_4$ ceramic s sintered at 1400 °C for 2 h exhibited good microwave dielectric properties, with ε_r = 9.88, $Q \times f$ = 131,445 GHz, tan δ = 6.85 × 10^{-5},and τ_f = −60 ppm/°C.

1. Introduction

Low-K microwave dielectric ceramic materials have long been studied as millimeter wireless communication systems [1–5]. It is required to possess low dielectric constant and high quality factor. This is crucial to advancing the properties of intelligent transport systems, excellent ultra-stable oscillators, and ultrahigh-speed wireless local area networks. Thus, many scientific and commercial attentions have been attracted to search for low-loss and low-cost dielectric ceramics for millimeter-wave applications.

The spinel structure, with general formula AB_2O_4 or $B(AB)O_4$ is adopted by various materials, including catalysts, superconductors, magnetic materials, semiconductors and microwave dielectric ceramics at millimeter region. M_2SnO_4 [6–10] and MAl_2O_4 [11–14] (M = Zn, Mg) have been reported for millimeter region application. Although, MGa_2O_4 (M = Zn, Mg) have been widely applied to catalysts [15,16], semiconductors [17,18], and phosphors [19,20], until 2013, MGa_2O_4 (M = Zn, Mg) [21–28] have been reported in microwave applications.

Researches have studied the dielectric properties of $ZnGa_2O_4$ [21–23], $MgGa_2O_4$ [24,25], and solid solutions such as Zn-substituted $MgGa_2O_4$ [26] and Zn $(Ga, Al)_2O_4$ [27]. As for Zn-substituted $MgGa_2O_4$ ceramics, the dielectric constant increased owing to the increasing ionic of the A-O bond in the tetrahedral 8a site [26]. And in (1-x) $ZnAl_2O_4$-$x$$ZnGa_2O_4$ solid solutions, Ga substitution for Al leads to a small negative τ_f. Crystal structure refinement was used to clarify the relationship between the crystal structure and the microwave dielectric properties of $MgGa_2O_4$ [25]. The partials inversion spinel $MgGa_2O_4$ ceramics with 0.86 inversion degree show greater microwave dielectric performance than samples with higher (0.88) or lower (0.84) inversion degree. Therefore, it can be concluded that the cation distribution may affect and improve the microwave dielectric performance of spinel ceramics.

$ZnGa_2O_4$ spinel ceramics have a low sintering temperature (1385 °C), a wide sintering temperature region, and good microwave dielectric properties. $ZnGa_2O_4$ is a typical normal spinel with Zn^{2+} occupying one-eighth of the tetrahedral interstices 8(a) and Ga^{3+} occupying half of the octahedral interstices 16(d) [21]. And $CuGa_2O_4$ is a typical inverse 2–3 spinel, and the configuration of inverse 2–3 spinel is $B(AB)O_4$ with 1/2 B^{3+} plus all A^{2+} occupying half of the octahedral interstices 16(d) and 1/2 B^{3+} occupying one-eighth of the tetrahedral interstices 8(a). Therefore to introduce inverse spinel structure, Cu-substituted $ZnGa_2O_4$ ceramics were applied to this study. The main focus of this paper is to study the effect of the cation distributions on microwave dielectric properties of Cu-substituted

* Corresponding author.
E-mail address: ngdzqt@163.com (Q. Zhang).

http://dx.doi.org/10.1016/j.ceramint.2017.07.104
Received 4 July 2017; Received in revised form 12 July 2017; Accepted 13 July 2017

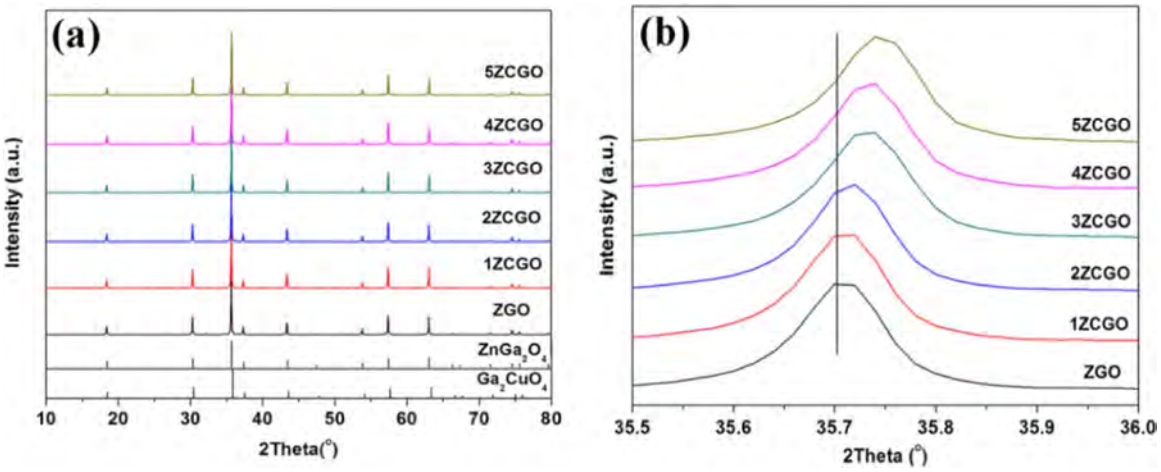

Fig. 1. XRD patterns (a) and their enlarged XRD patterns (b) of $Zn_{1-x}Cu_xGa_2O_4$ (x = 0–0.05) ceramics sintered at 1400 °C for 2 h in air.

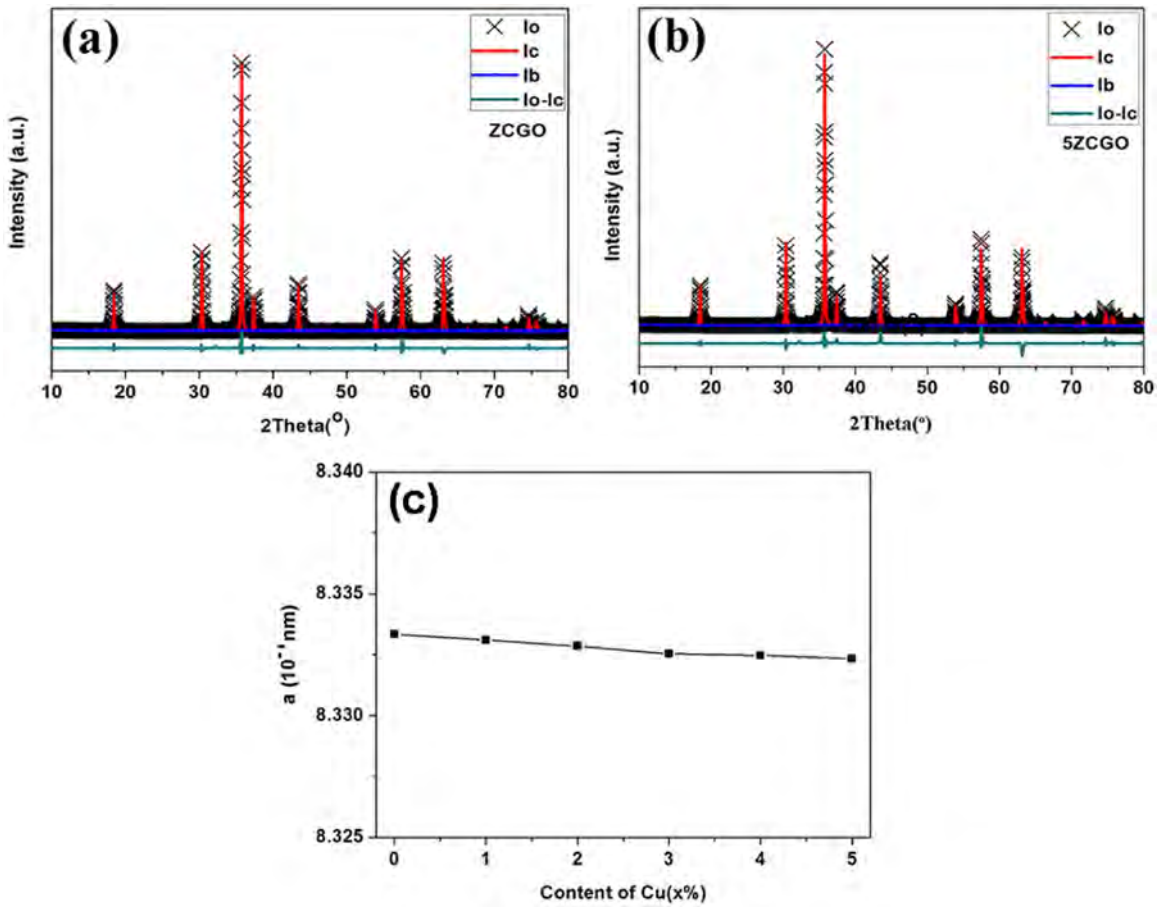

Fig. 2. Refined XRD pattern of $Zn_{1-x}Cu_xGa_2O_4$ fired at 1400 °C for 2 h (a) $ZnGa_2O_4$ (b) $Zn_{0.95}Cu_{0.05}Ga_2O_4$ (c) refined cell parameters a.

Table 1
Refined cell parameters of $Zn_{1-x}Cu_xGa_2O_4$ (x = 0–0.05) fired at 1400 °C for 2 h.

Content of Cu (%)	a (10^{-1} nm)	Vm (Å^3)	Degree of inversion	a_m
0	8.3334	72.34	0	12.97
1	8.3331	72.33		12.971
2	8.3329	72.33		12.972
3	8.3325	72.32		12.973
4	8.3325	72.32		12.974
5	8.3323	72.31	0.06	12.975

$ZnGa_2O_4$ spinel ceramics.

2. Experimental procedure

Solid solution of $Zn_{(1-x)}Cu_xGa_2O_4$ (x = 0–0.05) spinel ceramics were prepared via traditional solid state method. The analytical grade ZnO, CuO, and Ga_2O_3 were mixed on the basis of the stoichiometric compositions of $Zn_{(1-x)}Cu_xGa_2O_4$. The mixed powders were milled for 8 h with ethanol in polyethylene jars with agate balls in a planetary milling machine (QM-1SP4; Jialing, Nanjing, China). After dried at 100 °C for 24 h, the mixture were calcined at 1000 °C for 2 h. Then the treated powders were mixed with 7 wt% polyvinyl alcohol as adhesion

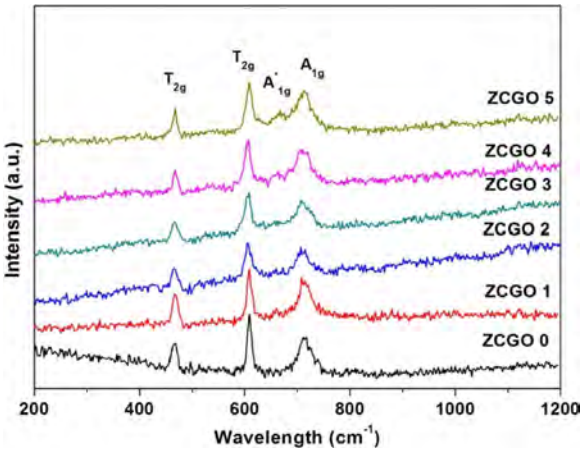

Fig. 3. Raman spectra of $Zn_{1-x}Cu_xGa_2O_4$ (x = 0–0.05), sintered at 1400 °C for 2 h in air.

agent and pressed into pellets of 13 mm in diameter and 6 mm in thickness with an automatic machine (DY-20; Tianjin Keqi Instrument, Tianjin, China) under 75 MPa. These pellets were sintered at 1250–1350 °C for 4 h in air with a high-temperature electric furnace (KSX4-16, Allfine, Wuxi, China).

The bulk density was analyzed by Archimedes' method and 5 samples were measured for every sintering temperature and give the average density. The polished samples were thermally etched to investigate the surface microstructure which was analyzed by a scanning electron microscope (SEM, Hitachi SU8010, Japan). Element analysis was carried out with an energy dispersive spectrometer (EDS, JSM-6510). XPS core-level spectra were taken with a X-ray photoelectron spectrometer (ESCALAB 250, Thermo Fisher, UK). The X-ray source was Al-K. The analyzer pass energy was kept fixed at 20 eV for all the scans. To clarify the effect of Cu substitution for Ga on the crystal structure of the ceramics, the crystal structures of crystalline phases were refined using the General Structure Analysis System (PC-GSAS) software. Regarding the Rietveld analysis, the XRD profiles of the ceramics were obtained by a step scanning method in the 2θ range of 5–80° with a step size of 0.02° and a counting time of 3.0 s/step. Raman spectra were excited with an argon laser (20 mw laser power) and recorded using a Raman spectrometer (HR800, Horiba Labram, 514 nm He-Cd laser, 20 mW laser power). Fourier transform infrared (FT-IR) spectroscopy were performed by NICOLET 5700 (Thermo, America). To investigate the microwave dielectric performance, ε_r, $Q \times f$, f_0 and τ_f were detected using cavity resonator method [28] by using Lightwave Component Analyzer (Hewlett Packard 8703 A, 1550 nm/130 MHz-20 GHz) and the resonator size is ϕ36 mm × h25 mm. The temperature coefficient of resonant frequency (τ_f) was calculated in the temperature range from 20 °C to 80 °C.

3. Result and discussion

Fig. 1 shows the XRD patterns of $Zn_{1-x}Cu_xGa_2O_4$ (x = 0–0.05) ceramics with x varied from 0 to 0.05, following sintered at 1400 °C for 2 h. Obviously, all the diffraction peaks could be well indexed to spinel structured $ZnGa_2O_4$ (JCPDS No.86-0413) or $CuGa_2O_4$ (JCDPS No.78-012) without creating a second phase. Although $ZnGa_2O_4$ and $CuGa_2O_4$ all belong to spinel compounds with the space group $Fd3m$, the structure of these two spinel compounds is a little different ($ZnGa_2O_4$ is a normal spinel and $CuGa_2O_4$ is an inverse spinel). Notably, the reflections of $Zn_{1-x}Cu_xGa_2O_4$ shifts to higher diffraction angles as x increased, especially the main diffraction peaks. The shift of reflections could be ascribed to the lattice contraction. And the refinement of the cell parameter could confirm the lattice contraction.

In fact the octahedral site preference energy (OSPE) of Cu^{2+} is 15.6 kcal/mol and 0 for Zn^{2+}. Therefore, based on the crystal field theory, Cu^{2+} cation preferentially occupies the octahedron site. Therefore, we predicted that the degree of inversion of $Zn_{1-x}Cu_xGa_2O_4$ (x = 0–0.05) ceramics equals to the content of Cu. To prove this prediction, the refinement of the crystal structure was applied. The crystal structures were refined to clarify the relationship between the cation distribution and Cu content. The crystal structure parameters of $ZnGa_2O_4$ (JCPDS No.86-0413) were used as the initial parameters for refinement of the crystal structure of the $Zn_{1-x}Cu_xGa_2O_4$ (x = 0–0.05) ceramics. The reliability factors R_{wp} and R_p of the Rietveld analysis were evaluated and the appropriate degree of inversion of the $Zn_{1-x}Cu_xGa_2O_4$ (x = 0–0.05) ceramics was decided. Fig. 2 shows the refined XRD pattern of $ZnGa_2O_4$ and $Zn_{0.05}Cu_{0.95}Ga_2O_4$ fired at 1400 °C for 2 h and refined cell parameter a. Table 1 summarizes cell parameter and inversion degree of $Zn_{1-x}Cu_xGa_2O_4$ (x = 0–0.05) ceramics sintered at 1400 °C for 2 h. The increase in inversion the degree suggests that Cu cation preferentially occupies the octahedron site.

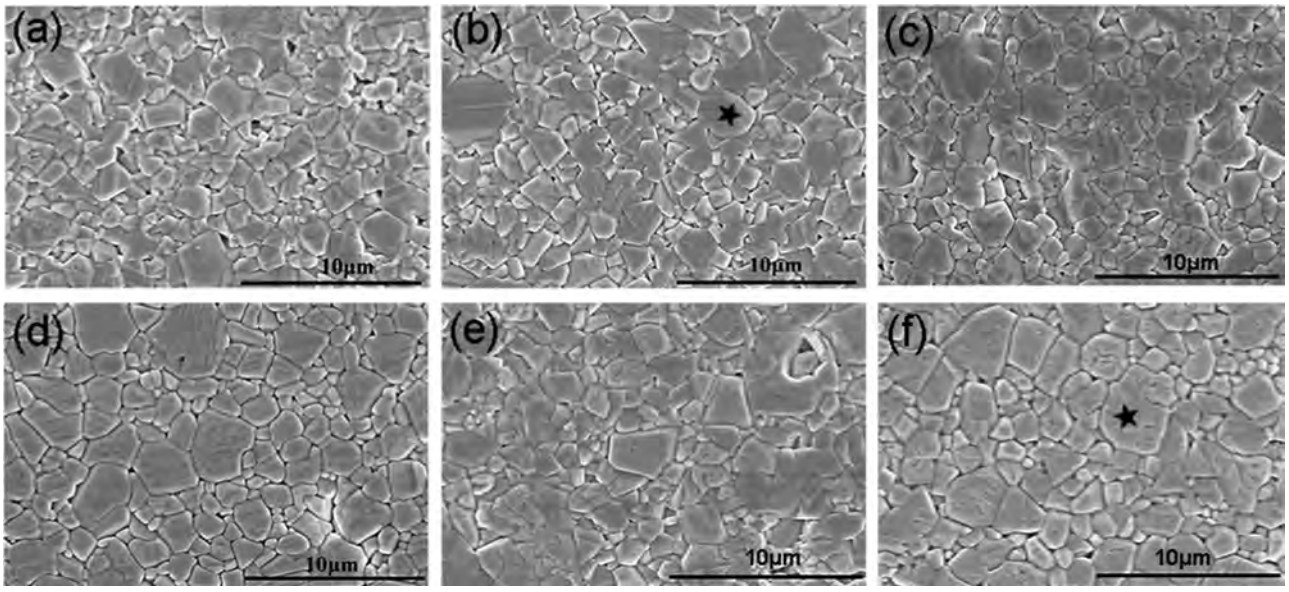

Fig. 4. SEM images of thermal etched surface of $Zn_{1-x}Cu_xGa_2O_4$ (x = 0–0.05) ceramics sintered at 1400 °C for 2 h in air: (a) x = 0;(b) x = 0.01;(c) x = 0.02;(d) x = 0.03; (e) x = 0.04; (f) x = 0.05,respectively.

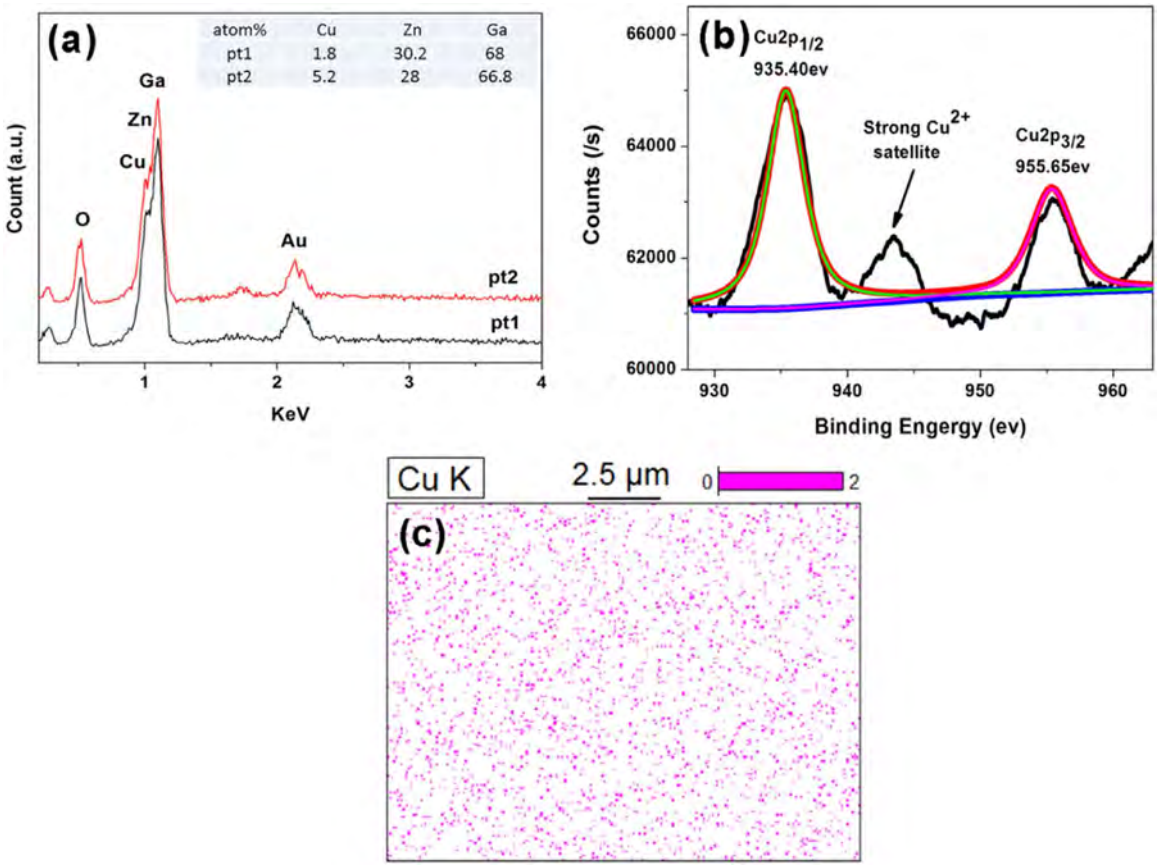

Fig. 5. (a)Energy dispersive spectrometer patterns corresponded to micro-areas marked in the SEM images, sintered at 1400 °C for 2 h in air (b) XPS spectrum of $Zn_{0.95}Cu_{0.05}Ga_2O_4$, sintered at 1400 °C for 2 h in air (c) Element scanning results of $Zn_{0.99}Cu_{0.01}Ga_2O_4$ (SEM(b)), sintered at 1400 °C for 2 h in air.

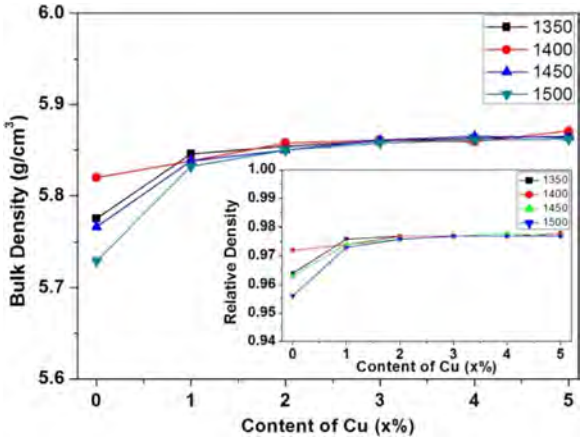

Fig. 6. The bulk densities and the relative densities of $Zn_{1-x}Cu_xGa_2O_4$ (x = 0–0.05) ceramics, sintered at temperatures range from 1350 °C to1500 °C for 2 h in air.

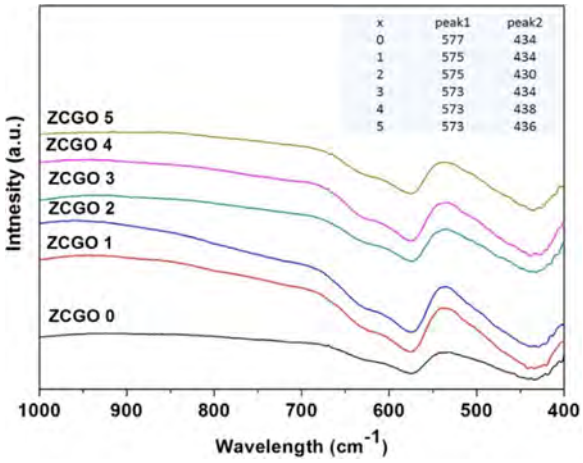

Fig. 7. FT-IR spectrum of $Zn_{1-x}Cu_xGa_2O_4$ (x = 0–0.05) ceramics, sintered at temperatures range from 1350 °C to1500 °C for 2 h in air.

Further proof of the cation distribution can be suggested by the data of Raman spectroscopy. The Raman spectra of $Zn_{1-x}Cu_xGa_2O_4$ consists of four distinct peaks at around 468 (T_{2g}), 607 (T_{2g}), 673 (A^*_{1g}), and 712 (A_{1g}) which are consistent with the Rafal J.Wglusz's research [29]. The presence of extra band associated with $A_{1\ g}$ mode (marked with an asterisk in Fig. 3) can be connected to the site inversion and has informative value for the direct recognition of an inverted spinel. Laguna-Bercero et al. [30] underlined the key role of asymmetry of the A_{1g} mode as a direct indication of the cationic tetrahedral-octahedral site inversion. In Fig. 3, $Zn_{1-x}Cu_xGa_2O_4$ clearly reveals significant site distortion with Cu substitution. A^*_{1g} mode could also give a frank image of the inversion degree. The rising intensity of A^*_{1g} mode

Table 2
Microwave dielectric properties of $Zn_{1-x}Cu_xGa_2O_4$ (x = 0–0.05) fired at 1400 °C for 2 h.

component	ε_r	f_0 (GHz)	tan δ (*10^{-5})	$Q \times f$ (GHz)
0ZCGO	9.85	9.02	10.51	85,824
1ZCGO	9.89	9.01	6.86	131,445
2ZCGO	9.92	9.00	6.98	128,914
3ZCGO	9.95	9.01	7.10	126,872
4ZCGO	9.98	9.00	7.43	121,098
5ZCGO	10	9.00	7.83	114,992

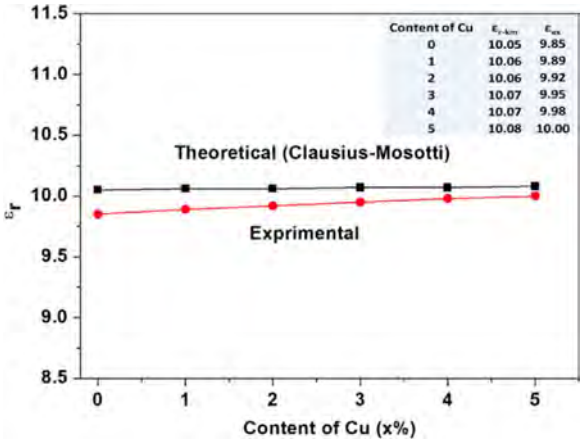

Fig. 8. Experimental and theoretical dielectric constant varied with Cu-substitution, sintered at temperatures range from 1350 °C to1500 °C for 2 h in air.

illustrated that the inversion degree climbed during Cu substitution.

SEM micrographs of $Zn_{1-x}Cu_xGa_2O_4$ (x = 0–0.05) ceramics sintered at 1400 °C are exhibited in Fig. 4. The average size kept steady during Cu-substitution. EDS patterns (Fig. 5(a)) gained at two positions marked with the star in Fig. 4 shows that the element compositions agreed with the stoichiometric ratio in $Zn_{0.99}Cu_{0.01}Ga_2O_4$ and $Zn_{0.95}Cu_{0.05}Ga_2O_4$. XPS spectrum of $Zn_{0.95}Cu_{0.05}Ga_2O_4$ in Fig. 5(b) indicates that Cu state in $Zn_{0.99}Cu_{0.01}Ga_2O_4$ is Cu^{2+}. An energy-disperse spectroscopy were measured on the $Zn_{0.95}Cu_{0.05}Ga_2O_4$ shown in Fig. 5(c) which confirmed that the Cu element almost equally distributed in $Zn_{0.99}Cu_{0.01}Ga_2O_4$ ceramics.

Fig. 6 shows that the bulk densities and relative densities of $Zn_{1-x}Cu_xGa_2O_4$ (x = 0–0.05) sintered at various temperatures from 1350 °C to 1500 °C for 2 h. The maximum bulk densities for $Zn_{1-x}Cu_xGa_2O_4$ were achieved at 1400 °C. Obviously, dense structure is good for the microwave dielectric performance. For each sintering temperature, the bulk density increased with the growing content of Cu. These results are due to the higher bulk density of the inverse-spinel $CuGa_2O_4$ (6.22 g/cm^3) than the normal-spinel $ZnGa_2O_4$ (5.99 g/cm^3). More interestingly, the relative densities of $Zn_{1-x}Cu_xGa_2O_4$ ceramics increases with x. Therefore, Cu-substitution of $ZnGa_2O_4$ could also densify $Zn_{1-x}Cu_xGa_2O_4$ ceramics.

Fig. 7 shows the FT-IR spectrum of $Zn_{1-x}Cu_xGa_2O_4$ (x = 0–0.05) ceramics sintered at 1400 °C for 2 h in air. The absorption peaks at around 577 cm^{-1} and 434 cm^{-1} represent the bond vibration of Zn–O–Ga and Zn–O. The shift of absorption bands in FT-IR spectrum is due to the differences of ion dielectric polarizability. The ion dielectric polarizability of Cu^{2+}, Zn^{2+} and Ga^{3+}, is 2.11, 2.04 and 1.50, respectively [31]. Due to the refined crystal structure and Raman spectrum data, Cu cation preferentially occupies the octahedron site. Therefore Zn–O–Ga and Zn–O bonds were partially substituted by Zn–O–Cu and Ga–O bonds. The higher ion dielectric polarizability of Cu^{2+} (substituted Ga^{3+}) resulted in the absorption peak at around 577 cm^{-1} shifting to lower wavenumber from 577 cm^{-1} to 573 cm^{-1}. And the lower ion dielectric polarizability of Ga^{3+} (substituted Zn^{2+}) resulted in the absorption peak at around 434 cm^{-1} shifting to higher wavenumber from 434 cm^{-1} to 436 cm^{-1}. Therefore, the FT-IR spectrum data could in turn confirming the results of refined XRD and Raman spectrum of $Zn_{1-x}Cu_xGa_2O_4$ (x = 0–0.05) ceramics.

Table 2 summarizes the microwave dielectric properties (ε_r, f_0, tan δ, $Q \times f$) of $Zn_{1-x}Cu_xGa_2O_4$ (x = 0–0.05), fired at 1400 °C for 2 h. The dielectric polarizabilities of ZnO, CuO and Ga_2O_3 are 4.01, 4.11and 8.96, respectively [31]. The dielectric polarizability differences resulted in the vibration of ε_r value as is shown in Fig. 7(b). α_m and Vm (as is shown in Table. 1) were estimated to illuminate the effects of Cu-substitution on the dielectric constant with the Clausius-Mossotti Eq. (1)

$$\varepsilon_r = [3/(1 - b\alpha_m/Vm)] - 2 \quad (1)$$

where Vm is the molecular volume, α_m is dielectric polarizability, and $b = 4\pi/3$. The theoretical values of dielectric constant were assessed with Eq. (1) and displayed in Fig. 8. The theoretical ε_r value climbed as Cu content increased. The experimental dielectric constant of $Zn_{1-x}Cu_xGa_2O_4$ shows a similar trend as the theoretical dielectric constant.

Fig. 9(a) displays $Q \times f$ values of $Zn_{1-x}Cu_xGa_2O_4$ (x = 0–0.05) sintered at temperatures from 1300 °C to 1500 °C. 1400 °C is the optimized sintering temperature for the highest relative density and $Q \times f$ values. The $Q \times f$ values of $Zn_{1-x}Cu_xGa_2O_4$ ceramics jumped to a maximum value of 131,445 GHz (x = 0.01) and then declined with Cu content. Surprisingly, in the temperature range (1350 °C–1500 °C), $Zn_{0.99}Cu_{0.01}Ga_2O_4$ achieved great $Q \times f$ values steadily. This indicates that $Zn_{0.99}Cu_{0.01}Ga_2O_4$ could obtain great $Q \times f$ values in a large sintering temperature range.

Fig. 9(b) exhibits the τ_f values of $Zn_{1-x}Cu_xGa_2O_4$ (x = 0–0.05) sintered at 1400 °C. The average τ_f value is about −60 ppm/°C. The factors that affect τ_f values are very complicated. Usually, τ_f value depends on the component, relative densities, microstructure and so on. In the x range (0–0.05), there is no significant shift of τ_f values. This result reveals that the τ_f value of $Zn_{1-x}Cu_xGa_2O_4$ (x = 0–0.05) is stable that we can use the same content of materials with large positive τ_f to obtain a series $Zn_{1-x}Cu_xGa_2O_4$ ceramics with near zero τ_f value

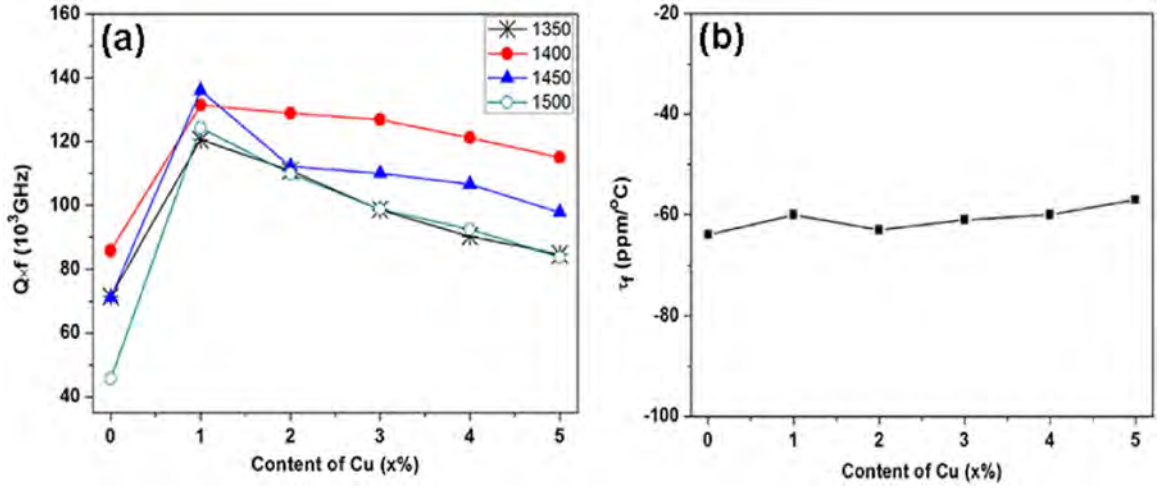

Fig. 9. (a) $Q \times f$ values of $Zn_{1-x}Cu_xGa_2O_4$ (x = 0–0.05) ceramics varied with sintering temperatures; (b) τ_f values of $Zn_{1-x}Cu_xGa_2O_4$ (x = 0–0.05) ceramics sintered at 1400 °C for 2 h in air.

4. Conclusions

We have successfully synthesized Cu-substituted $ZnGa_2O_4$ with good microwave dielectric properties. Cu^{2+} preferentially occupies the octahedron site and formed inverse spinel structure in normal-spinel structured $ZnGa_2O_4$, and caused lattice contraction. The rising intensity of A^*_{1g} mode in Raman spectrum and the refined crystal structure parameters illustrated that the inversion degree climbed with the growing content of Cu. The $Q \times f$ value of $Zn_{1-x}Cu_xGa_2O_4$ ceramics increased from 85,824 GHz to 131,445 GHz during Cu-substitution. The differences of ion dielectric polarizability caused the shift of absorption bands in FT-IR spectrum. Ion dielectric polarizability differences and cell volumes affected permittivity (ε_r) and increased ε_r slightly with Cu-substitution. The appropriate Cu content, degree of inversion, high relative densities resulted in higher $Q \times f$ value. Great microwave dielectric performance were achieved in $Zn_{0.99}Cu_{0.01}Ga_2O_4$ spinel ceramics with ε_r = 9.88, $Q \times f$ = 131,445 GHz, tan δ = 6.85 × 10^{-5},and τ_f = −60 ppm/°C. Due to the τ_f value of $Zn_{1-x}Cu_xGa_2O_4$ (x = 0–0.05) is stable, same content of materials with large positive τ_f can be applied to a series $Zn_{1-x}Cu_xGa_2O_4$ ceramics to adjust τ_f to near zero value. In summary, spinel-structured $Zn_{1-x}Cu_xGa_2O_4$ (x = 0–0.05) ceramics are promising candidate materials for millimeter-wave devices.

Acknowledgements

This work was supported by Priority Academic Program Development of Jiangsu Higher Education Institutions (PAPD), the Opening Project of the State Key Laboratory of High-Performance Ceramics and Superfine Microstructure (project No. SKL201309SIC), the College Industrialization Project of Jiangsu Province (JHB2012-12), the Jiangsu Collaborative Innovation Center for Advanced Inorganic Function Composites, the Science and Technology Projects of Guangdong Province (project No.2011A091103002), and Graduate student training innovation project in jiangsu province (KYCX17_0973).

References

[1] W. Wersing, Microwave ceramics for resonator and filters, Curr. Opin. Solid. State Mater. Sci. 1 (1996) 715–731.
[2] R.J. Cava, Dielectric materials for applications in microwave communications, J. Mater. Chem. 11 (2000) 54–62.
[3] M.T. Sebastian, Dielectric materials for wireless communication, J. Mater. Chem. 11 (2010) 54–62.
[4] S.B. Narang, S. Bahel, Low loss dielectric ceramics for microwave applications: a review, J. Ceram. Process. Res. 11 (3) (2010) 316–321.
[5] J.C. Kim, M.H. Kim, J.B. Lim, S. Nahm, J.H. Paik, J.H. Kim, Synthesis and microwave dielectric properties of $Re_3Ga_5O_{12}$, (Re: Nd, Sm, Eu, Dy, Yb, and Y) ceramics, J. Am. Ceram. Soc. 90 (2007) 641–644.
[6] Y.C. Chen, H.M. You, K.C. Chang, Influence of Li_2WO_4, aid and sintering temperature on microstructures and microwave dielectric properties of Zn_2SnO_4 ceramics, Ceram. Int. 41 (2014) 5257–5262.
[7] Y.C. Chen, M.Z. Weng, J.M. Hong, Effect of Zr substitution on microwave dielectric properties of Zn_2SnO_4 ceramics, Ceram. Int. 25 (2014) 5000–5005.
[8] (a) Y.C. Chen, J.M. Liou, M.Z. Weng, H.M. You, K.C. Chang, Improvement microwave dielectric properties of Zn_2SnO_4 ceramics by substituting Sn^{4+} with Ti^{4+}, Ceram. Int. 40 (2014) 10337–10342;
(b) Q. Ma, S.P. Wu, Y.X. Fan, Synthesis and microwave dielectric properties of Zn_2SnO_4 ceramics, Ceram. Int. 40 (2014) 1073–1080.
[9] Y.C. Chen, Y.N. Wang, C.H. Hsu, Elucidating the dielectric properties of Mg_2SnO_4 ceramics at microwave frequency, J. Alloy. Compd. 509 (2011) 9650–9653.
[10] Y.C. Chen, H.M. You, Microwave dielectric properties of $ZnO–B_2O_3–SiO_2$-doped Zn_2SnO_4 ceramics for application in triple bands inverted-U shaped monopole antenna, J. Alloy. Compd. 616 (2014) 356–362.
[11] W. Lei, W.Z. Lu, J.H. Zhu, F. Liang, D. Liu, Modification of $ZnAl_2O_4$ -based low-permittivity microwave dielectric ceramics by adding 2MO–TiO_2 (M=Co, Mg, and Mn), J. Am. Ceram. Soc. 91 (2008) 1958–1961.
[12] W. Lei, W.Z. Lu, D. Liu, J.H. Zhu, Phase evolution and microwave dielectric properties of $(1–x)ZnAl_2O_4–xMg_2TiO_4$ ceramics, J. Am. Ceram. Soc. 92 (2009) 105–109.
[13] C.L. Huang, C.Y. Tai, C.Y. Huang, Y.H. Chien, Low-loss microwave dielectrics in the spinel-structured $(Mg_{1-x}Ni_x)Al_2O_4$ solid solutions, J. Am. Ceram. Soc. 93 (2010) 1999–2003.
[14] S. Takahashi, A. Kan, H. Ogawa, Microwave dielectric properties and crystal structures of spinel-structured $MgAl_2O_4$ ceramics synthesized by a molten-salt method, J. Eur. Ceram. Soc. 37 (2016) 1001–1006.
[15] X. Chen, H. Xue, Z.H. Li, L. Wu, X.X. Wang, X.Z. Fu, Ternary wide band gap p-block metal semiconductor $ZnGa_2O_4$ for photocatalytic benzene degradation, J. Phys. Chem. C 112 (2008) 20393–20397.
[16] X.N. Zhang, J.H. Huang, K.N. Ding, Y.D. Hou, X.C. Wang, X.Z. Fu, Photocatalytic decomposition of benzene by porous nanocrystalline $ZnGa_2O_4$ with a high surface area, Environ. Sci. Technol. 43 (2009) 5947–5951.
[17] T. Ohtake, N. Sonoyama, T. Sakata, Electrochemical luminescence of $ZnGa_2O_4$ and $ZnGa_2O_4$:Mn semiconductor electrodes emission mechanism under cathodic and anodic polarization, Bull. Chem. Soc. Jpn. 72 (1999) 2617–2623.
[18] T. Ohtake, N. Sonoyama, T. Sakata, Luminescence dependence on imposing $ZnGa_2O_4$ activated with Mn^{2+} or Cr^{3+} n-type bias for $ZnGa_2O_4$ and semiconductor electrodes, Electrochem. Commun. 7 (2005) 1389–1392.
[19] S. Itoh, H. Toki, Y. Sato, K. Morimoto, T. Kishino, The $ZnGa_2O_4$ phosphor for low-voltage blue cathodoluminesence, Cheminformatics 138 (1991) 1509–1512.
[20] Y. Zhuang, J. Ueda, S. Tanabe, Enhancement of red persistent luminescence in Cr^{3+}-doped $ZnGa_2O_4$ phosphors by Bi_2O_3 codoping, Appl. Phys. Express 6 (2013) 2602.
[21] J. Xue, S. Wu, J. Li, Synthesis, microstructure, and microwave dielectric properties of spinel $ZnGa_2O_4$ ceramics, J. Am. Ceram. Soc. 96 (2013) 2481–2485.
[22] M.J. Lu, X. Ouyan, S.P. Wu, R.Y. Ge, R. Xu, A facile hydrothermal route to self-assembled $ZnGa_2O_4$ particles and their microwave application, Appl. Surf. Sci. 364 (2016) 775–782.
[23] M.M. Can, G.H. Jaffari, S. Aksoy, S.I. Shah, T. Firat, Synthesis and characterization of $ZnGa_2O_4$ particles prepared by solid state reaction, J. Alloy. Compd. 549 (2013) 303–307.
[24] S.P. Wu, J.J. Xue, R. Wang, J.H. Li, Synthesis, characterization and microwave dielectric properties of spinel $MgGa_2O_4$, ceramic materials, J. Alloy. Compd. 585 (2014) 542–548.
[25] A. Kan, T. Moriyama, S. Takahashi, H. Ogawa, Cation distributions and microwave dielectric properties of spinel-structured $MgGa_2O_4$ ceramics, Jpn. J. Appl. Phys. 52 (2013) 09KH01.
[26] A. Kan, S. Takahashi, T. Moriyama, H. Ogawa, Influence of Zn substitution for Mg on microwave dielectric properties of spinel-structured $(1-x)MgGa_2O_4$-$xZnGa_2O_4$, Jpn. J. Appl. Phys. 53 (2014) 09PB03.
[27] S. Wu, J. Xue, Y. Fan, Spinel $Mg(Al, Ga)_2O_4$ solid solution as high-performance microwave dielectric ceramics, J. Am. Ceram. Soc. 97 (2014) 3555–3560.
[28] X.C. Fan, X.M. Chen, X.Q. Liu, Complex-permittivity measurement on high-Q materials via combined numerical approaches, IEEE Trans. Microw. Theory 53 (2005) 3130–3134.
[29] R.J. Wiglusz, A. Watras, M. Malecka, P.J. Deren, R. Pazik, Structure evolution and up-conversion studies of ZnX^2O^4: Er^{3+}/Yb^{3+} (X = Al^{3+}, Ga^{3+}, In^{3+}) nanoparticles, Eur. J. Inorg. Chem. 6 (2014) 1090–1101.
[30] M.A. Laguna-Bercero, M.L. Sanjuan, R.I. Merino, Raman spectroscopic study of cation disorder in poly-and single crystals of the nickel aluminate spinel, J. Phys.-Condens. Matter 19 (2007) 186–217.
[31] R.D. Shannon, Dielectric polarizabilities of ions in oxides and fluorides, J. Appl. Phys. 73 (1993) 348–366.